

## Correlation of molecular orientation with adhesion at polystyrene/solid interfaces

Philip T. Wilson <sup>a</sup>, Lee J. Richter <sup>a,\*</sup>, William E. Wallace <sup>b</sup>,  
Kimberly A. Briggman <sup>c</sup>, John C. Stephenson <sup>c</sup>

<sup>a</sup> Surface and Microanalysis Science Division, National Institute of Standards and Technology, 100 Bureau Drive, Gaithersburg, MD 20899-0541, USA

<sup>b</sup> Polymers Division, National Institute of Standards and Technology, 100 Bureau Drive, Gaithersburg, MD 20899-8541, USA

<sup>c</sup> Optical Technology Division, National Institute of Standards and Technology, 100 Bureau Drive, Gaithersburg, MD 20899-8442, USA

Received 6 May 2002; in final form 12 July 2002

### Abstract

Vibrationally resonant sum-frequency generation (VR-SFG) has been used to characterize the molecular orientation of the phenyl groups at the interface between polystyrene (PS) films and surface-modified glass substrates. Both the interface structure and the film adhesion are found to vary as the substrate surface is changed from hydrophobic to hydrophilic. The improved adhesion on the hydrophilic substrate is attributed to the development of attractive hydrogen bonds between surface hydroxyl (OH) groups and the  $\pi$  electron cloud of the phenyl ring. This interaction is manifest by changes in the orientation distribution of the phenyl rings at the interface. Published by Elsevier Science B.V.

### 1. Introduction

Polymer/solid interfaces are critical to many applications including adhesives, protective coatings, lubricants, and composites. Polymer interfaces can differ considerably from the bulk in important characteristics such as glass transition temperature, end-group concentration, molecular mass distribution, amorphous/crystalline ratio and crosslink density [1]. Functional performance

characteristics, such as practical adhesion of thin films or tensile yield stress in composites depend in a complex fashion on both interface and bulk properties [2]. Nonetheless, there often is a clear relationship between functional performance and interface properties [2,3]. Substrate surface modification is an important tool for the optimization of polymer/solid interfaces. Rational interface design is hampered by the lack of molecular level diagnostics for buried interface structure. Buried interfaces are inaccessible to charged particle probes, and X-ray and neutron scattering techniques have limited interfacial sensitivity. We have used vibrationally resonant sum frequency

\* Corresponding author. Fax: +1-301-926-6689.

E-mail address: [lee.richter@nist.gov](mailto:lee.richter@nist.gov) (L.J. Richter).

generation (VR-SFG) spectroscopy to determine the molecular structure at the interface between a simple glassy polymer, polystyrene (PS), and a glass substrate as the substrate surface is modified from hydrophobic to hydrophilic. The orientation of the phenyl groups of PS,  $(\text{CH}_2\text{CHC}_6\text{H}_5)_n$ , as determined by VR-SFG spectroscopy, changes significantly with substrate modification. The orientation of the phenyl groups at a hydrophobic surface to which PS adheres poorly is very similar to the orientation of PS at the air interface. The orientation of the phenyl groups at a hydrophilic surface to which the film adheres more strongly is different, consistent with a polymer rearrangement driven by attractive interactions between the hydroxyl (OH) groups of the hydrophilic surface and the  $\pi$  electron cloud of the phenyl ring. This work demonstrates that we now have an in situ probe able to guide the optimal design of polymer/substrate interactions.

VR-SFG is a nonlinear vibrational spectroscopy in which one detects a visible photon created by the summation (SUM) of a resonant infrared (IR) photon and a typically nonresonant visible (VIS) photon. The mixing process is symmetry forbidden in the dipole approximation in centrosymmetric media such as liquids and noncrystalline solids, but allowed by the broken symmetry of an interface. Therefore, the spectroscopy is uniquely suited to the study of surfaces and interfaces [4]. When studying thin films, procedures must be developed to isolate the signal from the buried interface of interest from the signal due to the other surfaces in the system, such as the film free surface and the substrate backside surface. We have developed a thin film interference technique that, unlike total internal reflection VR-SFG [5–7], allows the study of buried interfaces between any two dielectric films, independent of the dielectric constant of the films [8].

## 2. Experimental

The films of interest, in this case a layer of spin-on-glass (SOG) and then a film of atactic

PS, are deposited on a Au mirror. The SOG films were formed by spin coating Dow Corning FOx-14®<sup>1</sup> at 2000 RPM from methyl isobutyl ketone solutions onto Au films ( $\sim 200$  nm thick) evaporated on Si wafers. The films were annealed at 300 °C in air for 1 h. The polymer thin films were atactic 220,000 number-average relative molecular mass PS, spin coated at 2000 RPM from toluene solutions and annealed under vacuum for 2 h at 120 °C. All PS and FOx film thicknesses were determined by spectrometric ellipsometry and are accurate to  $\sim 1$  nm. AFM studies of the glass prior to deposition of the PS determined an RMS roughness of 1.2 nm, while studies of the PS free surface determined an RMS roughness of 0.5–0.8 nm.

The experiments were performed with a broad-bandwidth SFG apparatus in which broadband ( $>150$   $\text{cm}^{-1}$  FWHM) 3  $\mu\text{m}$  IR pulses, derived from a  $\sim 100$  fs, 1 kHz, regeneratively amplified Ti-sapphire laser system, were temporally and spatially overlapped with narrow-bandwidth ( $\sim 3$   $\text{cm}^{-1}$ ) 794 nm (VIS) pulses at the sample. The reflected sum-frequency light was collected, dispersed in a 0.75 m spectrograph, and detected with a scientific grade CCD array detector. This allowed the simultaneous acquisition of a  $>300$   $\text{cm}^{-1}$  wide SFG spectrum. In this work, the IR and VIS pulse energy, beam diameter, and angle-of-incidence with respect to the surface normal were typically: 4  $\mu\text{J}$ , 100  $\mu\text{m}$ , 54° and 1  $\mu\text{J}$ , 150  $\mu\text{m}$ , 36° respectively. The displayed spectra were normalized by the response of a Au film covered with a perdeuterated PS film, which corrects for the intensity envelope of the broad-bandwidth IR pulse. All spectra are presented with the  $x$ -axis as the IR wavenumber, to allow easy comparison with linear vibrational spectroscopies.

<sup>1</sup> We identify certain commercial equipment, instruments, or materials in this article to specify adequately the experimental procedure. In no case does such identification imply recommendation or endorsement by the National Institute of Standards and Technology, nor does it imply that the materials or equipment identified are necessarily the best available for the purpose.

### 3. Results and discussion

The VIS and IR fields at the Au/SOG, SOG/PS, and PS/air interfaces are determined by interference between the incident and reflected beams. Similarly, the detected sum-frequency radiation is influenced by interference between direct and reflected paths. By appropriate choice of angle of incidence and film thickness, these interferences can be used to selectively probe either the free PS/air or buried SOG/PS interface [8]. Fig. 1 shows VR-SFG spectra from two Au/SOG/PS/air samples, one optimized for the PS/air surface, and one for the buried SOG/PS interface. The C-H stretching modes of the phenyl ring dominate the spectra in the 3000–3100  $\text{cm}^{-1}$  range displayed. The spectra are clearly different, establishing selectivity for different interfaces. This is confirmed by the spectra in Fig. 1 of the same samples after UV-ozone treatment of the free PS surface: the spectrum originating at the exposed PS/air interface is destroyed while that originating at the

buried interface is unaffected. UV irradiation and plasma treatment of PS free surfaces has been reported to disrupt aromatic SFG signals [9].

The signal in a VR-SFG experiment arises from the coherent superposition of radiation from resonant and nonresonant terms and can be expressed as [10]:

$$\text{Signal} \propto \left| B e^{i\varphi} + \sum_r \frac{A_r}{\nu - \nu_r + i\Gamma_r} \right|^2, \quad (1)$$

where  $\varphi$  is the relative phase between the vibrational resonances (frequency  $\nu_r$ , strength  $A_r$ , line-width  $\Gamma_r$ ) and the non-resonant background  $B$ . The reflection coefficients for the IR, VIS and SUM beams are included in  $B$ ,  $A_r$ , and  $\varphi$  [8]. The surface of Au has a strong non-resonant nonlinearity [11], completely dominating  $B$ . The vibrational resonances of the SOG or PS films may appear on this nonresonant background as positive, negative, or asymmetric Lorentzian features, depending on  $\varphi$ . From  $\varphi$  one may determine

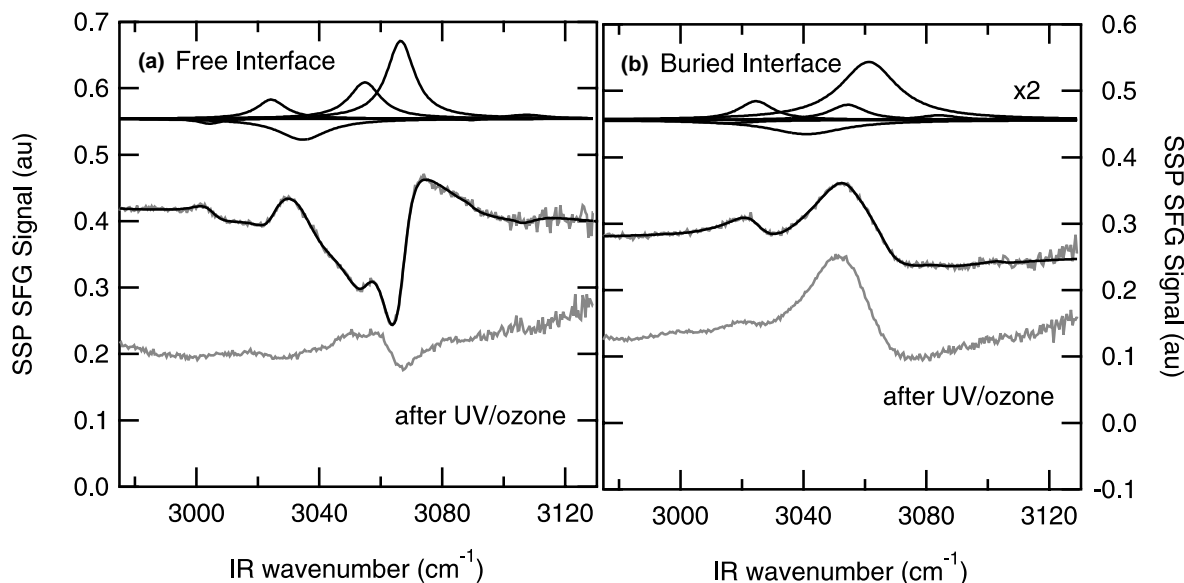


Fig. 1. VR-SFG spectra (gray) before and after UV-ozone treatment of the free surface. (a) Sample optimized for study of the free interface (129 nm PS film on a 198 nm SOG film). (b) Sample optimized for study of the buried interface (129 nm PS film on a 330 nm SOG film). The lines through the data (black) are fits to the model described in the text. The imaginary parts of the resonant components of the fits are also shown offset above the data. All spectra were recorded in a SSP configuration: the detected SUM and incident VIS pulses were polarized perpendicular to the plane of incidence ( $S$ ), i.e. with the electric vector maximized in the surface plane, and the IR pulse was polarized in the plane of incidence ( $P$ ), i.e. with electric vector components both in the surface plane and along the surface normal. The spectra after UV-ozone treatment have been displaced for clarity.

whether a particular transition dipole vector points toward or away from the Au surface [12]. In Fig. 1 the spectra prior to ozone treatment are fit to the form of Eq. (1). The fits include seven resonant lines for each interface, five fundamental modes and two combination bands, [13] and account for minor contributions to the spectra by the excluded interface. Also shown are the imaginary parts of the resonant components for the dominant interface; these show the frequency,  $\nu_r$ , width,  $\Gamma_r$ , and the strength and sign of  $A_r$  for each vibrational resonance. The three principal features in the spectrum of the free surface appear at 3024, 3035, and 3067  $\text{cm}^{-1}$  and can be assigned to the  $\nu_{20B}$ ,  $\nu_{7A}$ , and  $\nu_2$  normal modes of mono-substituted benzene [14].<sup>2</sup> The SFG spectrum of the free PS/air surface of PS films spun on silica [9,13] has been carefully characterized. The spectrum in Fig. 1 agrees with these previous reports. At the free surface of PS, the phenyl rings point away from the film, into the air, with a tilt angle  $\theta \sim 60^\circ$  from the surface normal [13]. Recent simulations of the PS free surface [15] are consistent with these measurements, and suggest that the order of the phenyl groups extends  $\sim 1$  nm into the film.

The differences between the spectra of the buried interface in Fig. 1 and the free interface are mostly due to the different phase  $\varphi$ : the free surface features reflect destructive interference with the Au non-resonant background, while the buried interface features arise from constructive interference. This indicates that the buried interface has a vector orientation *opposite* that of the free surface; i.e. at the buried interface, the phenyl groups point toward the Au (and the SOG). Thus at both interfaces (buried and free), the phenyl groups point away from the bulk of the PS film. There is a notable shift in the frequency of the fully symmetric CH stretch ( $\nu_2$ ) between the free surface 3067  $\text{cm}^{-1}$  and both the buried interface

3062  $\text{cm}^{-1}$  and the bulk 3060  $\text{cm}^{-1}$ . This is consistent with the determination that the phenyl groups point out into the air and the observation that  $\nu_2$  of gas phase toluene is  $\sim 9 \text{ cm}^{-1}$  blue shifted with respect to the condensed liquid phase [16]. The bulk-like frequency of  $\nu_2$  at the buried interface spectra is consistent with confinement at the solid/solid interface. The strong similarity of the relative amplitudes of the fit components to the buried interface spectrum in Fig. 1 indicates that the orientational distribution at the buried interface is very similar to that at the free surface. However, the linewidths for the components of the buried interface are consistently broader than observed at the free surface, suggestive of greater heterogeneity [8].

Having established that we are observing the buried PS/SOG interface, and that for untreated SOG, the PS/SOG buried interface is similar to the PS/air surface, we now consider modified SOG surfaces. The SOG, FOx-14®, is a hydrogen silsesquioxane (HSQ) with composition  $\text{HSiO}_{1.5}$ . Water contact angles<sup>3</sup> on unmodified films were  $95^\circ$ , indicative of a hydrophobic surface. UV-ozone treatment of the SOG film for times greater than  $\sim 5$  min resulted in a hydrophilic surface, with water contact angles  $\theta_w$  less than  $6^\circ$  (see Fig. 2a). The hydrophobic nature of the unmodified SOG is attributed to a surface layer of silicon hydride (Si–H) groups. VR-SFG of the SOG films confirms the presence of surface Si–H (see Fig. 2b). The two strong features in the VR-SFG spectra at 2284 and 2275  $\text{cm}^{-1}$  agree well with the IR spectra of small HSQ molecules adsorbed on  $\text{SiO}_2$  [17]. The low  $\theta_w$  for the UV-ozone treated surface indicates that the Si–H termination is replaced by Si–OH consistent with the decrease in Si–H SFG signal. We estimate a surface hydroxyl coverage of  $\sim 5 \text{ nm}^{-2}$  based on  $\theta_w$  studies of quartz surfaces [18]. The UV-ozone treatment only affects the surface of the SOG. IR absorption studies of the

<sup>2</sup> In our earlier work [13] the feature at 3024  $\text{cm}^{-1}$  was assigned to 20A based on the ordering of the modes in ab initio calculations. This assignment is not consistent with the relative intensity of the features in the IR spectrum. The feature at 3024  $\text{cm}^{-1}$  has been reassigned to one component of a resonance between 20B and the combination bands 19B+8A and 19A+8B. The reassignment is consistent with [14] and [9].

<sup>3</sup> All contact angles were measured on sessile drops, within  $\sim 5$  s of contact of the liquid to the surface. Water contact angles on the FOx were observed to irreversibly decrease with time. This is attributed to hydroxylation of the surface Si–H groups by the water.

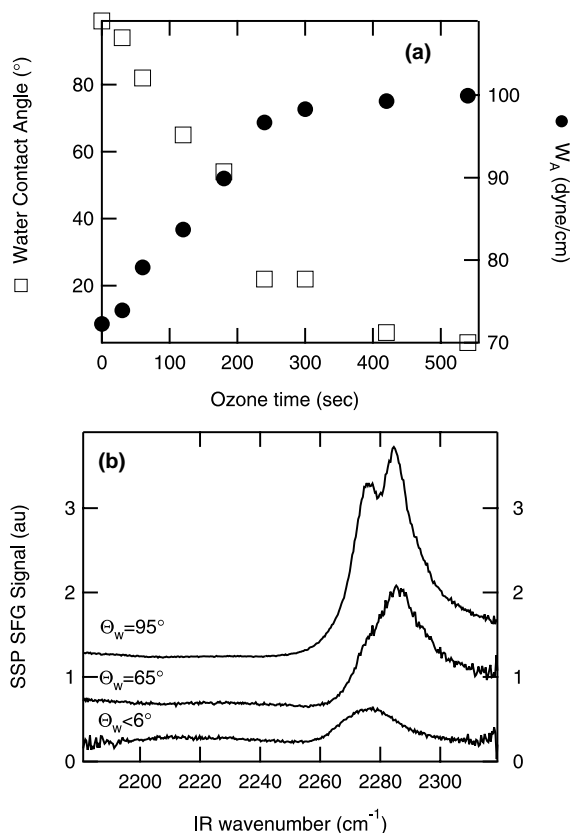


Fig. 2. (a) Water contact angle  $\Theta_w$  for the SOG film as a function of exposure to UV/ozone ( $\square$  left axis). Also shown is the calculated work of adhesion for the PS/SOG interface ( $\bullet$  right axis). (b) SFG spectra of the UV-ozone modified SOG film as a function of  $\Theta_w$ , showing a decrease in surface Si–H with increasing hydrophilicity.

bulk of the film indicated less than a 1% change in Si–H content. Additionally, atomic force microscopy (AFM) measurements indicated negligible change in the surface RMS roughness upon UV-ozone treatment.

The practical adhesion of the PS to the SOG directly correlated to the SOG hydrophilicity. The PS/hydrophobic SOG interface failed adhesively in 90° peel tests [19], while the PS/hydrophilic SOG interface passed the peel test. The results of the peel tests are in qualitative agreement with the work of adhesion,  $W_A$ , of the PS/SOG interface as shown in Fig. 2a. The polar and dispersive components of surface tension of PS and the SOG were determined from contact angle measurements with

water and diiodomethane;  $W_A$  was calculated from a geometric mean model of the interface tension [20]. The increase in  $W_A$  arises due to the development of polar (hydrogen bonding, dipole–dipole, induction, and acid–base) interactions between the modified surface and the PS film. There is little change in the strength of the dispersion interactions with treatment.

The structure of the polymer/glass interface varied significantly with the hydrophilicity of the SOG surface, as shown in the VR-SFG spectra in Fig. 3. There is a marked change in the relative strength of the feature due to  $\nu_2$  with respect to that of  $\nu_{20B}$  between the hydrophobic and hydrophilic substrates. The SFG spectrum of PS on UV-ozone modified SOG ( $\Theta_w < 6^\circ$ ) in Fig. 3 is very similar to the spectrum of PS at a PS/sapphire interface [7] suggesting that the spectrum may be characteristic of hydrophilic surfaces. Attempts to quantify the orientational distribution for the phenyl groups on the hydrophilic substrate based on the procedure of [13] failed, as the data was inconsistent with all possible narrow distributions of  $\psi$  and  $\theta$ . This assumed that PS phenyl groups had  $C_{2v}$  symmetry and normal modes that were independent of phenyl orientation. Since this approximation is inadequate to explain the present data, we have simulated the SFG spectra based on density functional theory (DFT) calculations<sup>4</sup> for isopropylbenzene, taken to approximate PS. As described below, DFT calculations show that some of the normal modes nominally associated with the phenyl ring depend significantly on the torsional angle of the phenyl with respect to the isopropyl backbone. Proper accounting for this enables the change in structure of PS on the ozone-treated SOG to be determined.

The strength of the observed SFG spectra depend on the vector projection of the molecular hyperpolarizability  $\beta$  on the electric field vectors of the laser beams (accounted for in  $A_r$ ). As in polarization sensitive infrared and Raman spectroscopy, this is the source of the ability of SFG to

<sup>4</sup> The calculations were performed with GAUSSIAN 98 (Revision A.9), [M. J. Frisch et al., Gaussian, Inc., Pittsburgh PA, 1998] using the B3LYP functional and a 6-31G\*\* basis set.

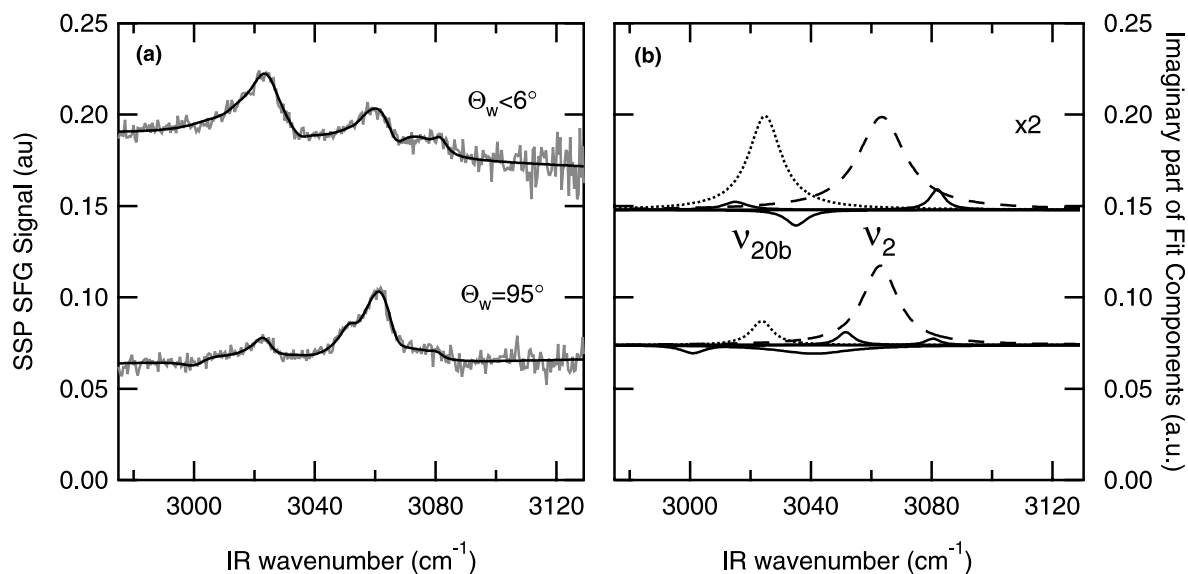


Fig. 3. (a) SFG spectra of the buried interface for unmodified (hydrophobic) and UV-ozone modified (hydrophilic) SOG substrates. The lines through the data are fits to the model described in the text. (b) The imaginary part of the resonant components of the fits. The components for  $\nu_{20B}$  (···) and  $\nu_2$  (---) are as labeled.

determine molecular alignment. When neither the SUM nor VIS frequencies are near resonances in the molecule,  $\beta$  can be approximated by

$$\beta_{ijk} = \frac{1}{2} \frac{\alpha_{ij}\mu_k}{(\nu - \nu_r + i\Gamma_r)}, \quad (2)$$

where  $\alpha$  is the dynamic Raman polarizability, and  $\mu$  the infrared transition dipole moment of vibrational mode  $r$  [21]. For the simulations  $\alpha$  and  $\mu$  are taken from the DFT calculations while  $\nu_r$  and  $\Gamma$  are taken from the fits to the data.  $\beta$  is expressed in the frame of reference  $x', y', z'$  of the phenyl ring (see Fig. 4), while the fields are expressed in laboratory fixed coordinates  $x, y, z$ .  $A_r$  (Eq. (1)) is then calculated for a distribution in which  $\theta$  (angle between  $z'$  and  $z$ ) is fixed and  $\varphi$  (precession of  $z'$  about the  $z$  axis) is isotropic. For  $\theta > 0$ , twists of  $\psi$  about the  $z'$  axis result in tipping the chain in and out of the plane of the interface ( $x$ – $y$  plane). At  $\theta$  near  $90^\circ$ ,  $\psi = \pm 90^\circ$  places the chain backbone perpendicular to the interface plane and is unphysical. Therefore  $\psi$  is averaged from  $-45^\circ$  to  $45^\circ$ .

In Fig. 4a are the simulated VR-SFG spectra for the calculated ground-state of isopropylben-

zene, in which the phenyl torsion angle  $\zeta = 0$ . Note that with  $\zeta = 0$ , at no value of  $\theta$  is the strength of  $\nu_{20B}$  comparable to that of  $\nu_2$ . Also note that the amplitude of  $\nu_{20B}$  is of opposite sign as  $\nu_2$ . The weakness of  $\nu_{20B}$  is to be expected based on the IR and Raman spectra of bulk PS [13]:  $\nu_{20B}$  has negligible Raman cross section, while  $\nu_2$  is prominent in both the IR and Raman spectra. The weakness of  $\nu_{20B}$  is also consistent with the reported VR-SFG spectra of other mono-substituted phenyl rings: phenylsiloxane, [13] thiophenol [22], and benzoate [23]. However, it was found that the calculated  $\beta$  depends strongly upon  $\zeta$ . Shown in Fig. 4b are simulated VR-SFG spectra in which  $\zeta = 30^\circ$ . The simulated spectra for  $\theta \sim 50^\circ$ , are in qualitative agreement with the spectra in Fig. 3:  $\nu_{20B}$  is strong, and of the same phase as  $\nu_2$ . The sensitivity of  $\beta$  to  $\zeta$  arises from the lowering of the symmetry of the ring, as evidenced by the H displacement patterns for the calculated normal modes shown in Fig. 4. The approximations used in calculating the spectra in Fig. 4 (neglect of the Fermi resonance in the calculated  $\beta$ , use of the simple perturbation expansion expression for  $\beta$ , use of a finite basis set in the calculations, etc.) are

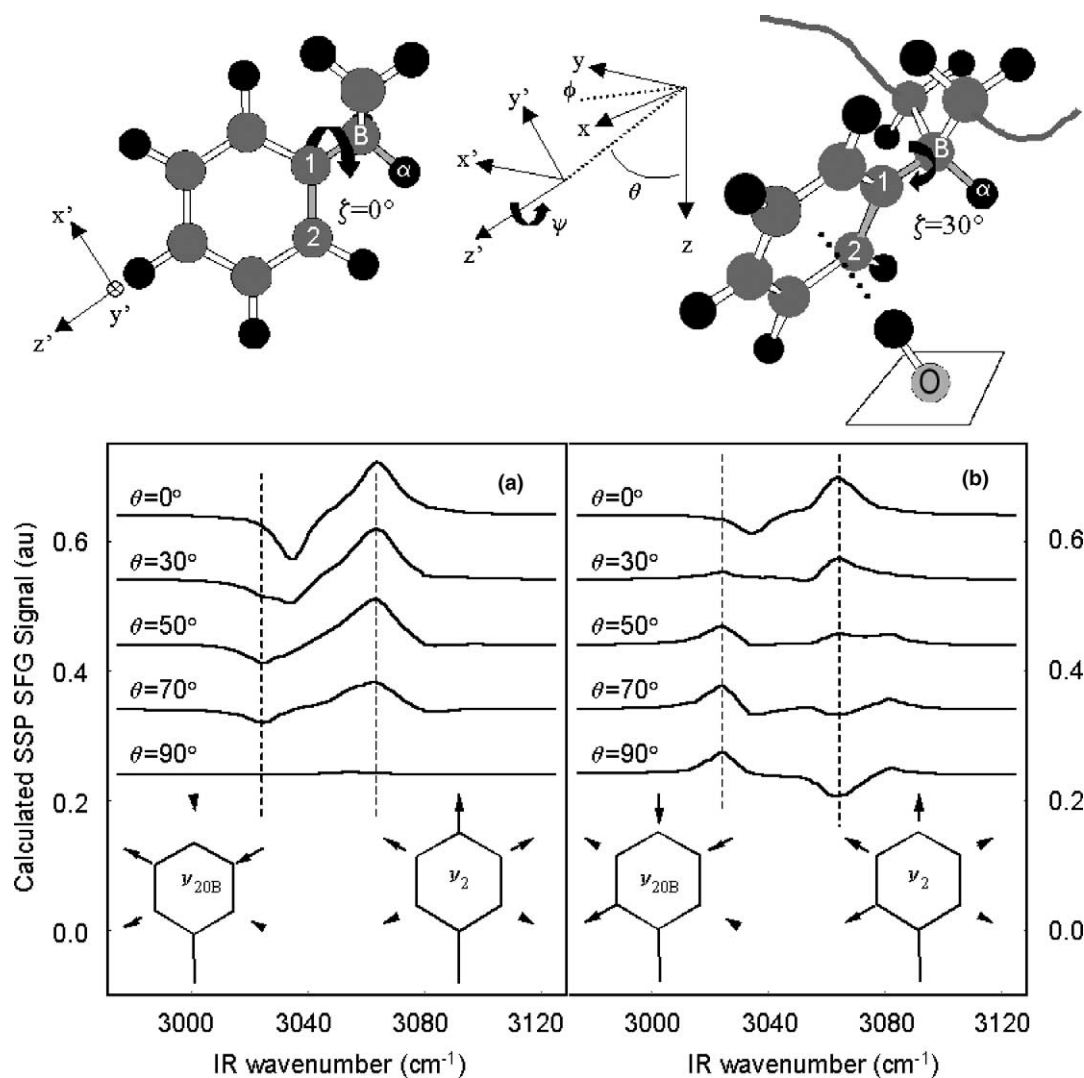


Fig. 4. Calculated SFG spectra for polystyrene with a ring torsion angle  $\zeta = 0^\circ$  (a) and  $\zeta = 30^\circ$  (b). The illustrations depict isopropylbenzene with  $\zeta = 0^\circ$  (left) and  $\zeta = 30^\circ$  (right). The H-bond between the  $\pi$  electron cloud of the phenyl ring and a surface OH is depicted schematically for  $\zeta = 30^\circ$ . The coordinate system of the phenyl ring ( $x', y', z'$ ), the torsion angle  $\zeta$ , and the Euler angles ( $\theta, \phi, \psi$ ) between the ( $x', y', z'$ ) frame and the laboratory frame ( $x, y, z$ ) are also shown. Color scheme is H, black; C, dark gray; O light gray. The three bonds defining the torsion angle  $\zeta$  are highlighted in light gray. The heavy dark gray lines in the right illustration indicate the polymer backbone.

such that quantitative determination of the orientational distribution is not merited. However the qualitative differences in the modeled spectra present a compelling case that the hydrophilic interface is composed of phenyl rings at  $\sim 50^\circ$  tilt angles with  $\sim 30^\circ$  torsional angles with respect to the backbone.

The torsion of the phenyl ring with respect to the chain backbone is reasonable for the hydrophilic substrate. In the benzene–water dimer [24], the most favorable configuration for  $\pi$ -hydrogen bonding is with the H centered on the  $\pi$  system of the ring, and the OH bond nominally perpendicular to the ring. This suggests an interface struc-

ture with the ring plane close to parallel with the substrate, allowing  $\pi$ -hydrogen bonding with the substrate OH. This favors large values of  $\psi$  and  $\theta$ . As stated above, the chain backbone must lie in the plane of the surface, thus the ring  $\cdots$ HO interaction will torque the ring away from the preferred configuration of  $\zeta = 0^\circ$ . The attractive interaction of benzene [25] with a single OH of  $10.2 \text{ kJ mol}^{-1}$  is approximately equal to the calculated torsional barrier of  $10.0 \text{ kJ mol}^{-1}$ . This observation supports the model of the PS orientation on the hydrophilic SOG, since the H-bond formation is capable of providing the energetic driving force for the reorganization.

The interplay between polymer self-interactions and polymer–substrate interactions that determine the interface structure is complex. This is demonstrated by the behavior of the related polymer poly-4-hydroxystyrene ( $\text{CH}_2\text{CHC}_6\text{H}_4\text{OH}$ )<sub>n</sub>, PHS. One might expect that the buried interface of PHS on hydrophilic glass would show extensive polar order due to the strong hydrogen bond between the polymer OH and the substrate. However, in preliminary measurements, the buried interfaces of PHS on both hydrophilic and hydrophobic substrates exhibit no polar order. This suggests that the PHS self-interaction is sufficiently strong to produce an amorphous interface, even in the presence of a substrate shown to order PS. These results demonstrate the importance of in situ diagnostics for the interfaces between polymers and engineered substrates. VR-SFG can provide the experimental data necessary for understanding the relationship between microscopic molecular order and macroscopic functional properties.

### Acknowledgements

Philip Wilson is a NIST National Research Council postdoctoral research associate.

### References

- [1] J. Schultz, M. Nardin, in: A. Pizzi, K.L. Mittal (Eds.), *Handbook of Adhesive Technology*, Marcel Dekker, New York, 1994, Chapter 2.
- [2] B. Pukanszky, E. Fekete, *Adv. Poly. Sci.* 139 (1998) 109.
- [3] K. Kendall, *Science* 263 (1994) 1720.
- [4] Y.R. Shen, *Nature* 337 (1989) 519.
- [5] S.R. Hatch, R.S. Polizzotti, S. Dougal, P.J. Rabinowitz, *J. Vac. Sci. Technol. A* 11 (1993) 2232.
- [6] J.C. Conboy, J.L. Daschbach, G.L. Richmond, *J. Phys. Chem.* 98 (1994) 9688.
- [7] K.S. Gautam, A.D. Schwab, A. Dhinojwala, D. Zhang, S.M. Dougal, M.S. Yeganeh, *Phys. Rev. Lett.* 85 (2000) 3854.
- [8] P.T. Wilson, K.A. Briggman, W.E. Wallace, J.C. Stephenson, L.J. Richter, *Appl. Phys. Lett.* 80 (2002) 3084.
- [9] D. Zhang, S.M. Dougal, M.S. Yeganeh, *Langmuir* 16 (2000) 4528.
- [10] R. Superfine, J.Y. Huang, Y.R. Shen, *Phys. Rev. Lett.* 66 (1991) 1066.
- [11] D.A. Koos, G.L. Richmond, *J. Phys. Chem.* 96 (1992) 3770.
- [12] R.N. Ward, P.B. Davies, C.D. Bain, *J. Phys. Chem.* 97 (1993) 7141.
- [13] K.A. Briggman, J.C. Stephenson, W.E. Wallace, L.J. Richter, *J. Phys. Chem. B* 105 (2001) 2785.
- [14] G. Varsanyi, *Vibrational Spectra of Benzene Derivatives*, Academic Press, New York, 1969.
- [15] T.C. Clancy, J.H. Jang, A. Dhinojwala, W.L. Mattice, *J. Phys. Chem. B* 105 (2001) 11493.
- [16] N. Fuson, C. Garrigou-Lagrange, M.L. Josien, *Spectrochim. Acta* 16 (1960) 106.
- [17] J. Eng et al., *J. Chem. Phys.* 108 (1998) 8680.
- [18] R.N. Lamb, D.N. Furlong, *J. Chem. Soc., Faraday Trans.* 1 78 (1982) 61.
- [19] 90° Peel tests were performed with Scotch 810 tape (Footnote 1).
- [20] S. Wu, *Polymer and Interface Adhesion*, Marcel Dekker, New York, 1982, Chapter 3.
- [21] C. Hirose, N. Akamatsu, K. Domen, *J. Chem. Phys.* 96 (1992) 997.
- [22] R. Braun et al., *J. Chem. Phys.* 110 (1999) 4634.
- [23] R.N. Ward, D.C. Duffy, G.R. Bell, C.D. Bain, *Mol. Phys.* 88 (1996) 269.
- [24] S.Y. Fredricks, K.D. Jordan, T.S. Zwier, *J. Phys. Chem.* 100 (1996) 7819.
- [25] A. Courty et al., *J. Phys. Chem. A* 102 (1998) 6590.